International Journal of Pharmaceutics 419 (2011) 107–113

Contents lists available at ScienceDirect

International Journal of Pharmaceutics

journal homepage: www.elsevier.com/locate/ijpharm

Characterization of melt extruded and conventional Isoptin formulations using Raman chemical imaging and chemometrics

Balázs Vajna*, Hajnalka Pataki, Zsombor Nagy, István Farkas, György Marosi

Department of Organic Chemistry and Technology, Budapest University of Technology and Economics, Budafoki út 8., H-1111 Budapest, Hungary

ARTICLE INFO

Article history:
Received 7 February 2011
Received in revised form 14 July 2011
Accepted 15 July 2011
Available online 23 July 2011

Keywords:
Micro-Raman
Hyperspectral imaging
Chemometrics
Pharmaceutical
MCR–ALS
Extrusion

ABSTRACT

Isoptin SR-E (Meltrex®) extruded tablets were assumed in a recent paper to be prepared with a composition different from a conventional (Isoptin SR) formulation. This study reveals, however, using Raman mapping and chemometric evaluation, that in fact the same composition, comprising Na alginate as polymer matrix, is used in both products. It means that only the difference in the manufacturing technology causes the reported sustained release of verapamil hydrochloride even in ethanol containing dissolution media. The products are compared based on the obtained Raman chemical images, which allowed concluding in a new structure-based explanation for the differences in the dissolution profiles in the presence of ethanol. It is also shown that extrusion technology influences the dissolution profile effectively, even in the cases when solid solution is formed only partially.

1. Introduction

Chemical imaging (CI) and chemometrics is a rapidly emerging combination to characterize pharmaceutical products. This family of analytical methods couples a vibrational spectrometric (mid-infrared, near-infrared or Raman) technique with appropriate optics (Šašić, 2010), enabling the acquisition of visualized images of the samples containing chemical information. There are a vast number of combinations for the different spectrometric techniques and sampling methods (e.g. point-by-point mapping and global imaging), which are extensively described in numerous recent review papers (Gowen et al., 2008; Gendrin et al., 2008a; Amigo, 2010; Gordon and McGoverin, 2010). All CI techniques create separate vibrational spectra corresponding to each point of the analysed surface, the dataset of which is processed then to provide image of the spatial distribution of the components.

When formulations under development or final products are subjects of such an analysis, a wide range of attributes can be characterized. Numerous solid dispersions have been studied, where the aim was to distribute the API homogeneously in a polymer matrix (Breitenbach et al., 1999; Nagy et al., 2010) and to keep the drug in stable amorphous phase (Docoslis et al., 2007; Karavas et al., 2007; Furuyama et al., 2008). The physical morphology of the active (or any other) ingredient in multicomponent formulations can be determined this way with high sensitivity (Lin et al., 2006). Most frequently the spatial distribution of a certain component is studied for troubleshooting of manufacturing processes (Clarke, 2004), monitoring blend homogeneity (Ravn et al., 2008) or to reveal the internal structure (Šašić et al., 2004; Šašić, 2007) and understand the physical attributes of the products (Chan et al., 2003). Based on the spatial distribution of the ingredients, various formulations of the same composition can be compared (Vajna et al., 2010) and counterfeit products can be distinguished from the original (Puchert et al., 2010).

The primary motivation of the present study arose on the basis of a recent paper published by Roth et al. (2009). The authors of the mentioned paper investigated the dissolution characteristics of different formulations containing verapamil hydrochloride, one of which was manufactured via melt extrusion (Meltrex®) technology. The extruded product, named Isoptin SR-E, was compared to the conventional sustained release Isoptin SR formulation. It was stated in the paper, that Isoptin SR-E (melt extruded) contained verapamil hydrochloride in a hydroxypropylcellulose (HPC) and hypromellose (HPMC) matrix, while Isoptin SR (sustained release) contained verapamil hydrochloride in a natrium-alginate retarding agent. This change in the excipients posed the most significant difference between the two products. The SR-E formulation was found to keep its dissolution characteristics unchanged even in dissolution media of high (40%) ethanol concentration, while the other conventional verapamil formulations (including Isoptin SR) lost their capability for sustained release under these circumstances.

The aim we intended to achieve by the determination of the real composition of the extruded pharmaceutical, was two-fold: (1) to demonstrate the fact that the pure spectrum and the

* Corresponding author. Tel.: +36 1 463 5918; fax: +36 1 463 3648.
E-mail address: balazs.vajna@gmail.com (B. Vajna).

0378-5173/$ – see front matter © 2011 Elsevier B.V. All rights reserved.
doi:10.1016/j.ijpharm.2011.07.023

spatial distribution of unknown components can be determined using Raman mapping and chemometrics, thus pharmaceuticals can be successfully characterized even if the prior information about the components is wrong or missing; and (2) to compare the tablets prepared with the two manufacturing technologies and to interpret their earlier reported (Roth et al., 2009) different behaviour based on their real composition and structure. (As the dissolution properties had been fully evaluated in the cited paper, this analytical approach does not aim to provide detailed physical and pharmacological comparison of the two Isoptin products.)

2. Materials and methods

2.1. Materials

The Isoptin SR-E 240 mg product, manufactured with melt extrusion (Meltrex®) was obtained from Abbott Laboratories Sp. z.o.o., Poland. The sustained release Isoptin SR 240 mg product was obtained from Abbott Laboratories, S.A.

2.2. Raman mapping experiments

Raman mapping spectra were collected using a Horiba Jobin-Yvon LabRAM system coupled with an external 785 nm diode laser source and an Olympus BX-40 optical microscope. Objectives of 10× and 100× magnification were used for optical imaging and spectrum acquisition. The laser beam is directed through the objective, and backscattered radiation is collected with the same objective. The collected radiation is directed through a notch filter that removes the Rayleigh photons, then through a confocal hole and the entrance slit onto a grating monochromator (950 groove/mm) that disperses the light before it reaches the CCD detector. All spectra were obtained at multiple spectrograph positions providing a spectral range of 260–2000 cm^{-1} and 3 cm^{-1} resolution.

The tablets were broken in two parts and Raman mapping was performed on the broken surface of the tablets. No milling, microtomy or such sample preparation was applied in order to avoid alteration of the original sample structure. The low resolution maps were collected with 10× objective (laser spot size: ~4 μm) and 10 μm step size, while 100× magnification (laser spot size: ~1 μm) and 2 μm step size were used when creating high resolution images. In each experiment the acquisition time of a single spectrum was 3 s and 20 spectra were averaged at each spatial position. The measured area, when the 10× objective was used, varied from 24 × 24 to 28 × 28 pixels. Maps recorded with the 100× objective consisted of 24 × 24 pixels.

The reference Raman spectra of the pure ingredients were also collected with both 10× and 100× objectives using sufficient acquisition times to achieve adequate signal-to-noise ratio (the actual measurement time depended on the materials themselves).

2.3. Data analysis

Before chemometric evaluation, all spectra were base-line corrected. (This was done by piecewise linear base-line correction using the same baseline points for all the maps and reference spectra.) The measured spectra were then normalized to unit area in order to eliminate the intensity deviation between the measured points. The raw three-dimensional data was unfolded into a 2-dimensional matrix (for the procedure see Gordon and McGoverin, 2010).

The estimation of pure component spectra from the Raman maps was carried out by multivariate curve resolution–alternating least squares (MCR–ALS, Jaumot et al., 2005). This technique is based on the following bilinear model:

$$\mathbf{X} = \mathbf{C}\mathbf{S}^{\mathrm{T}} + \mathbf{E} \quad (1)$$

$\mathbf{S}^{\mathrm{T}}$ ($k \times \lambda$) is the set of reference (pure component) spectra, $\mathbf{X}$ ($p \times \lambda$) is the matrix containing the mapping spectra, and $\mathbf{C}$ ($p \times k$) contains the vectors of spectral concentrations (each row in $\mathbf{C}$ contains the concentrations of the k ingredients). The matrix $\mathbf{E}$ represents the residual noise. If the spectra of the pure components are known, the $\mathbf{C}$ matrix can be calculated in a straightforward way with the classical least squares calculation, using $\mathbf{X}$ and $\mathbf{S}^{\mathrm{T}}$. This is comprehensively described in numerous papers (Gendrin et al., 2008a; Gowen et al., 2008; Gordon and McGoverin, 2010). If some or all of the components are unknown, MCR–ALS can be used, which itself generates both the concentration matrix $\mathbf{C}$ and pure spectrum matrix $\mathbf{S}^{\mathrm{T}}$ from the dataset $\mathbf{X}$ in an iterative manner, using an initial estimation for either $\mathbf{C}$ or $\mathbf{S}^{\mathrm{T}}$ and appropriate physical constraints. Easy to use programs are available from the developers (Jaumot et al., 2005) and in commercial software. All of these have internal algorithms for providing the initial estimations and the iterations afterwards, and require minimal effort from the user.

Non-negativity, closure and contrast constraints were used in our study. Non-negativity constraint comes from the logical expectation that negative values are meaningless for both concentrations and spectral intensities (de Juan and Tauler, 2006). Closure constraint forces the calculated spectral concentrations to give a sum of 1 for each pixel. Contrast constraint forces the subsequent pure component spectra to be as different from one another as possible and to have no overlapping peaks (Windig and Keenan, 2011). Another constraint has also been developed especially for hyperspectral chemical imaging applications (de Juan et al., 2008), which, however, was not needed to be used in the present study.

All calculations were performed in MATLAB 7.6.0 (Mathworks, USA) with PLS_Toolbox 6.0.1 and MIA_Toolbox 2.0.1 (Eigenvector Research, USA). Spectral library search was carried out by SpectralID 3.03 (Thermo Electron Corporation, USA). Other curve resolution and factor analysis methods are also available, but only MCR–ALS was used, as numerous studies have proven it to be the best choice for this purpose (Duponchel et al., 2003; Zhang et al., 2005; Gendrin et al., 2008b; Vajna et al., in press).

Spectral concentrations of the ingredients present in the sample (further also referred to as 'Raman scores' in order to avoid confusion with real concentrations) were computed with the same algorithm described above.

Visualization of spectra and spectral concentration maps was carried out with LabSpec 5.41 (Horiba Jobin Yvon, France). The statistical properties of scores (mean, standard deviation) were computed with MATLAB.

3. Results and discussion

Alterations in the dissolution profiles of differently manufactured formulations are usually explained by the differences in the chemical composition. However, it is generally more convenient if changes in the dissolution behaviour can be achieved through structural modification, just by applying another preparation method. Detailed analysis and adequate evaluation methods are required to determine, which one of these two factors is more relevant in a particular case. In order to understand the differences between the extruded Isoptin SR-E and the conventional Isoptin SR formulations, Raman chemical imaging was used. Preliminary investigations showed that the information about the constituents given in a former paper (Roth et al., 2009) was misleading. Therefore, multivariate exploratory (chemometric) evaluation was applied, i.e. instead of trying to find pure reference spectra the

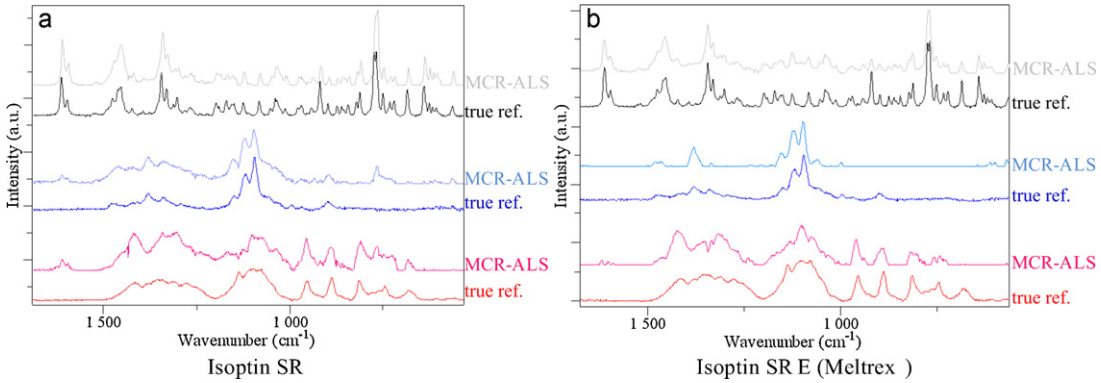

Fig. 1. Resolved spectra of major components in the two formulations compared to the corresponding reference spectra.

pure spectrum of each component was resolved from the Raman chemical images of these products.

As a first step, the measured Raman maps were evaluated via MCR–ALS to estimate the spectra of the pure components. These pure component spectra were then identified based on our spectral library. The spectral concentrations, estimated with the chemometric curve resolution methods, were then re-folded to a two-dimensional image according to the spatial position of each measured point. These distribution maps for each component were used to compare the internal structure of the two formulations, Isoptin SR and SR-E.

3.1. Estimated pure component spectra

Fig. 1a shows the estimated pure component spectra for Isoptin SR. It can be seen, that, in good agreement with (Roth et al., 2009), its three major components are verapamil hydrochloride, Na alginate and microcrystalline cellulose. In contrast, not the expected results were obtained upon the investigation of Isoptin SR-E formulation, in which, according to Fig. 1b, the same components were identified as in Isoptin SR. This means that instead of HPC and HPMC, which were stated in Roth et al. (2009), Na alginate was used as a polymer matrix in the Isoptin SR-E (Meltrex®). In addition, it can be seen by comparing Fig. 1a and b that the same polymorph of verapamil hydrochloride can be detected in the two formulations, as no significant difference can be seen between the resolved Raman spectra taken from the chemical images of Isoptin SR and SR-E. However, the determination of the amount of this crystalline form in the two products needed further investigation.

In order to make the observed composition more clear the polymer spectrum resolved with MCR–ALS has been compared to the Raman spectra of cellulose derivatives and Na alginate. This comparison is shown in Fig. 2.

Fig. 2 shows clearly that the resolved polymer spectrum cannot correspond to any of the given cellulose derivatives, but resembles the Na alginate signal instead. This implies that the stability of the verapamil HCl dissolution rate even at high ethanol content is a consequence of the structural changes caused by the applied extrusion method instead of the differences in the polymer matrices (for the matrices are the same in the two formulations).

Another issue to be mentioned concerns the difference in the performance of the spectrum resolution method in the two cases. In the case of the Isoptin SR formulation, MCR–ALS yielded good quality spectra for each component using only non-negativity and closure constraints. (Non-negativity means that all intensity values in the spectra and all concentrations must be 0 or higher. Closure means that the sum of the component concentrations have to be 1 in each measured pixel.) In contrast, worse results were achieved with regular MCR–ALS from the Raman map of Isoptin SR-E, as the

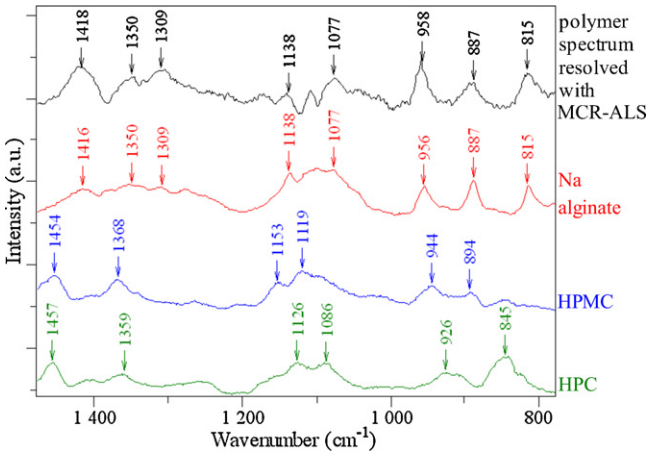

Fig. 2. Comparison of polymer spectrum resolved via MCR–ALS method with Na alginate, HPMC and HPC reference spectra.

predicted pure spectrum of Na alginate was significantly contaminated with certain peaks of the API (major bands at 1615, 1456, 1347 and 771 cm^{-1} are shown in Fig. 3). This phenomenon is due to the so-called rotational ambiguity in the spectral datasets (Rajkó and István, 2005) and already implies, even without seeing the spectral concentration maps, that their concentration distribution is correlated i.e. solid solution was formed to a certain extent.

Based on recent theoretical discussions (Tauler, 2001; Rajkó and István, 2005; Rajkó, 2009; Jaumot and Tauler, 2010) a new method has recently been introduced (Windig and Keenan, 2011)

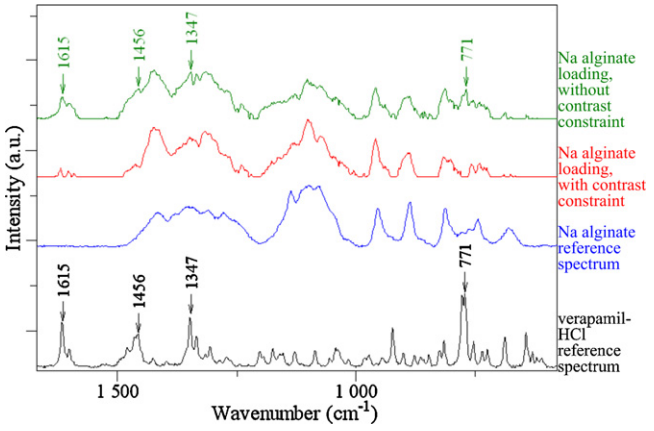

Fig. 3. Na alginate loadings predicted with MCR–ALS with and without applying contrast constraints, compared to library reference spectra.

which was applied here to solve the problem mentioned above. A new type of constraint (called 'contrast'), related to a convergence criterion developed earlier (Gan and Hopke, 2003), forces the iterative calculations to converge in spectra that are as much different from each other as possible (within the range of feasible mathematical solutions). Fig. 3 shows that applying this constraint in the iterations almost completely eliminates the API peaks and only negligible signals remain. Removing the API peaks from the Na-alginate loading, using this contrast constraint, is important to create reliable visualized spectral concentration (score) maps. (It should be noted that the library reference spectra of the API and Na alginate have a correlation coefficient of 0.06, thus, there is no, or very small, ambiguity due to spectral similarities. Such low correlation coefficient justifies the proper use of contrast constraint in this case.)

3.2. Comparison of Raman score maps of the two formulations

All pure spectrum resolution techniques are capable of giving estimation for the spatial distribution maps of all detected components as well. The calculated Raman scores (i.e. spectral concentrations) were refolded into a 2-way image and are shown in Fig. 4.

Fig. 4 shows the prominent differences in the distribution of components between the extruded Isoptin SR-E and the conventional sustained-release Isoptin SR formulations, inspected at 10× magnification. It can be seen that moderately heterogeneous distribution can be observed for all components in the conventional Isoptin SR tablet. Since this product is manufactured with wet granulation method (Roth et al., 2009), it can be assumed that the active ingredient does not completely dissolve during the granulation

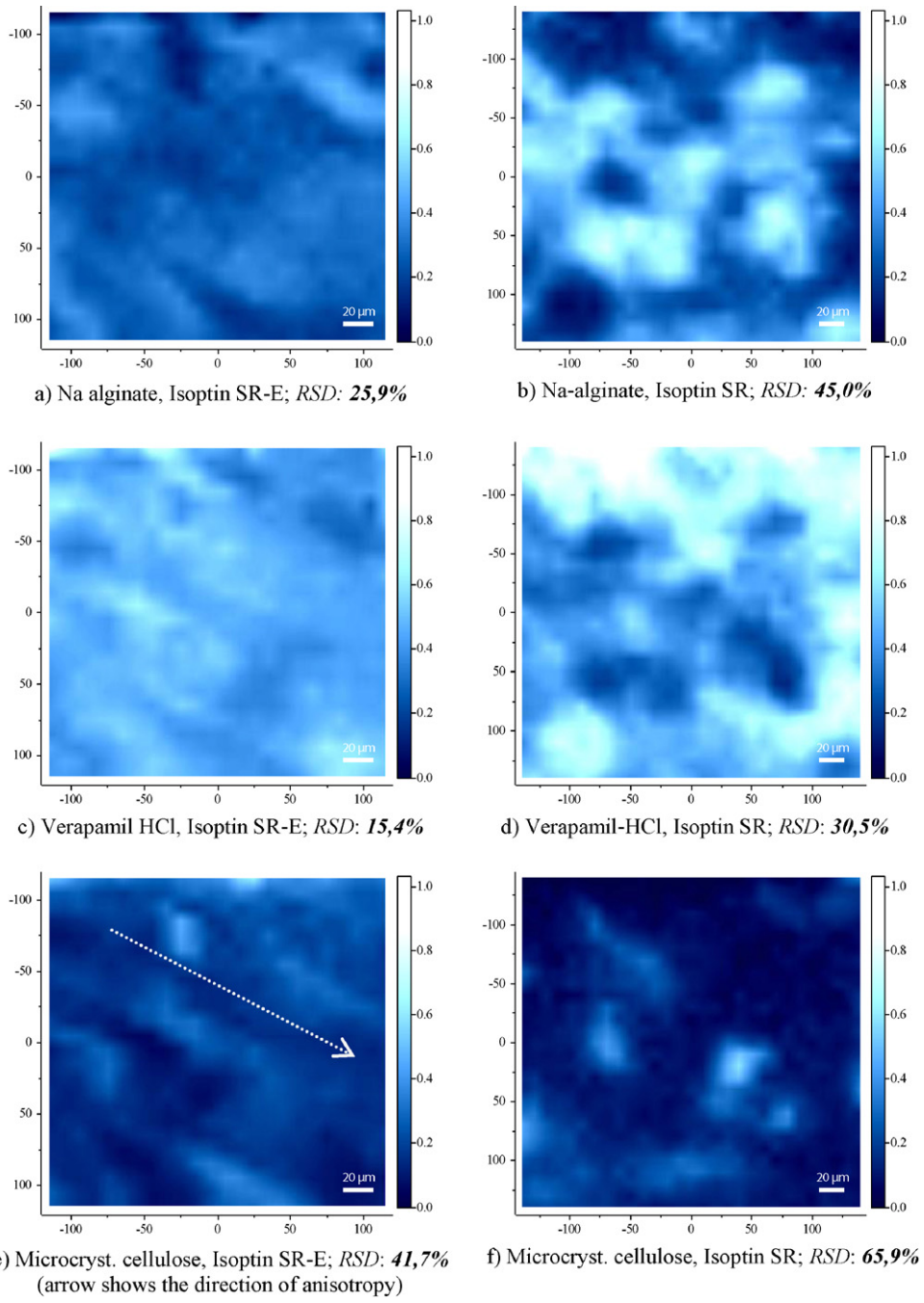

Fig. 4. Distribution maps of major components in the extruded Isoptin SR-E and the sustained-release Isoptin SR formulation (at 10× magnification).

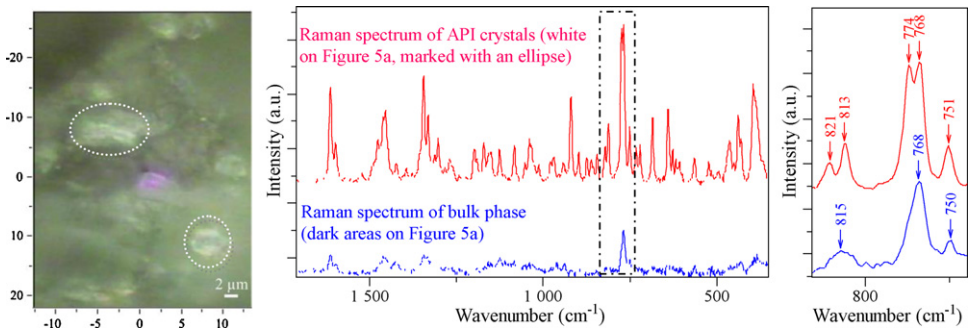

Fig. 5. (a) Optical microscopic image of the extruded Isoptin SR-E formulation at 100× magnification; (b) Raman spectra of bulk phase (lower) and API crystals (upper); and (c) Raman spectra of bulk phase (lower) and API crystals (upper) in the 745–825 cm^{-1} region.

procedure, as it has low water solubility at neutral pH environment (Streubel et al., 2000). In contrast, the extrusion process results in almost homogeneous API and Na alginate distribution as the applied mechanical shearing forces are more effective than wet granulation in this case. The heterogeneity of microcrystalline cellulose decreased as well because of the same reason.

The relative standard deviations (RSD) of the scores within a Raman map describe the distribution of the components numerically. Lower standard deviation of the spectral concentrations within the Raman score map corresponds to more homogeneous distribution of the respective ingredient (Gendrin et al., 2008a; Amigo, 2010; Vajna et al., 2010). The RSD values (given in Fig. 4) confirm the more homogeneous distribution of all three major components in the extruded product. Slight heterogeneities in Fig. 4a, c, and e are arranged in an anisotropic way, which can be explained by the orientation effect (shown with an arrow) of the extrusion process (the objects are wide in one direction).

The micro-Raman analysis performed with 10× magnification distinguished the products of different procedures from each other, however, slight inhomogeneity within the samples could not be detected this way. Further investigations were also carried out with 100× magnification to determine whether the active ingredient forms mostly solid solution with the Na alginate, or the majority of the API is in crystalline form.

In order to evaluate the heterogeneity of the ingredients at higher spatial resolution, optical microscopy (Fig. 5a) and single point spectrum acquisitions (Fig. 5b) were performed with 100× magnification. This analysis proved that several micrometers sized

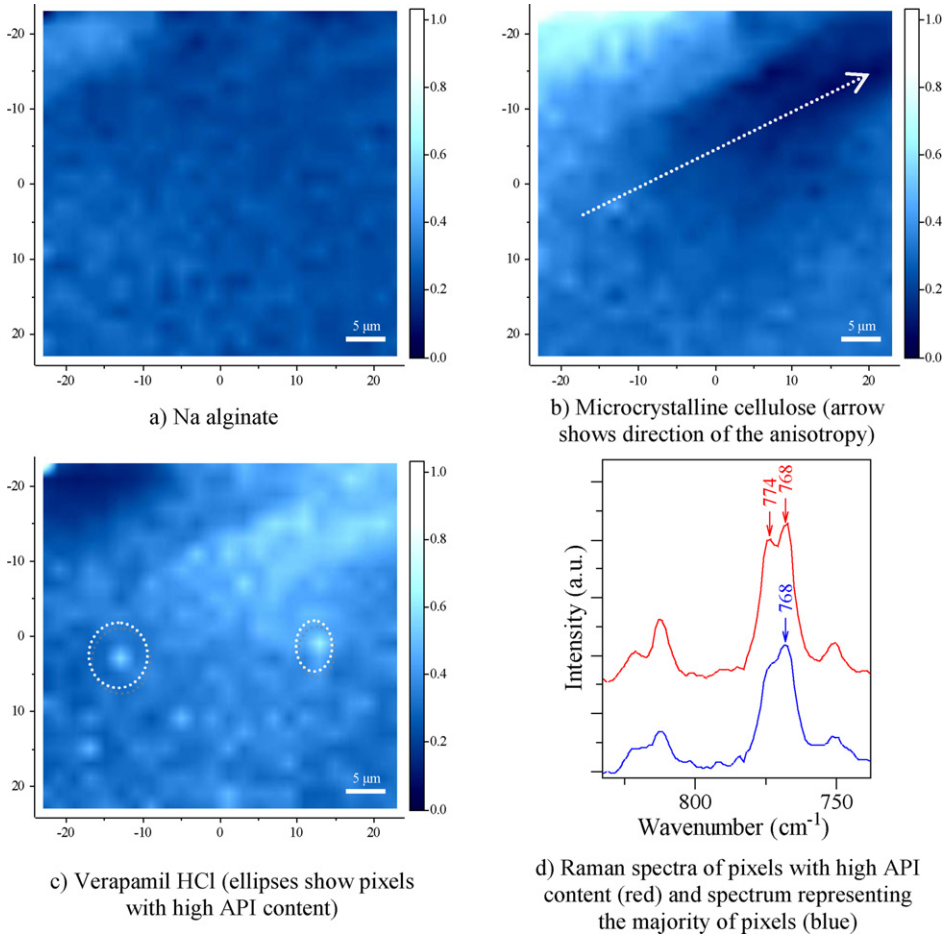

Fig. 6. Distribution maps of major components in the extruded Isoptin SR-E formulation at 100× magnification and representative Raman spectra of selected points.

API crystals (some of which marked by an ellipse in Fig. 5a) are present in the extruded sample, while the majority of the verapamil HCl (at low intensity sodium alginate rich areas) shows amorphous spectra (Fig. 5b and c). Significant band widening and merging is shown in Fig. 5c regarding the characteristic API peaks at 768 cm^{-1} and 815 cm^{-1} due to the amorphization. This implies that not the whole amount of the API forms molecular dispersion in the matrix polymer. Another possibility is that slow crystallization started after the extrusion process.

Optical microscopy and single point measurements alone are not sufficient to draw general conclusions. Due to surface roughness characteristics, chemically homogeneous areas may look heterogeneous in the optical microscopic images and vice versa. Consequently, Raman mapping was carried out, using 100× magnification, in areas which seemed homogeneous on the optical microscopic images, in order to determine whether the solid dispersion is perfectly formed in these areas.

Fig. 6 shows the distribution maps at 100× magnification (obtained with MCR–ALS method) from a seemingly crystal-free area on the optical microscopic image. The Isoptin SR-E sample looks fairly homogeneous for Na alginate and verapamil HCl, however, small deviations in the scores of the latter can be observed at certain pixels (examples of which are marked with an ellipse on Fig. 6c). Visual inspection of mapping spectra confirms that in these points the API signals have significantly higher intensities than in the nearby regions. In these points, both peaks of the crystalline API are detected (768 and 774 cm^{-1}). The majority of the pixels exhibit amorphous characteristics (one broad peak at 768 cm^{-1}), however, the second crystalline peak at 774 cm^{-1} can already be slightly detected as a 'shoulder' on the broad amorphous band. This shows that some small API crystals are also present in regions where the API generally forms solid dispersion with the alginate matrix. Additionally, the anisotropic features shown in Fig. 4a, c, and e can be observed at high spatial resolution as well (marked with an arrow in Fig. 6b).

The results shown above help to explain the observations described in the study written by Roth et al. (2009). On one hand, the extrusion process leads to the partial incorporation of amorphous API into a solid solution (or dispersion of colloid dimensions). The formation of this structure, via the high shear in the extruder, results in the observation that the dissolution of verapamil does not change significantly even when higher amount of ethanol is present in the dissolution media described in the cited paper. On the other hand, some of the active ingredient remained/transformed in the form of small, few or sub-micron-sized crystals. This means that although not all of the verapamil could be properly incorporated into the matrix, the small crystals are better protected by the Na alginate environment in the extruded form than in the conventional Isoptin SR tablet, in which the distribution of all components is heterogeneous.

4. Conclusions

This study demonstrates the applicability of the combined approach of Raman mapping and chemometric evaluation in the detailed characterization of pharmaceuticals, even if no prior information is given about the components, or, as in this case, the given information is wrong. The pure spectra of the major ingredients can be estimated from the Raman maps using appropriate chemometric methods. By comparing these spectra with the one present in adequate spectral libraries, the true ingredients of the tablets can be identified. It was proven, using MCR–ALS method, that the same polymer matrix is present in the extruded Isoptin SR-E (Meltrex®) sample as in the conventional sustained-release Isoptin SR formulation (in contrast to a recently published paper).

The spatial distribution maps of each identified ingredient can also be estimated with the chemometric methods shown in this study, which shows that the internal structure of unknown pharmaceuticals can be revealed without any prior information about the samples.

These score maps were used to compare the internal structure of the two formulations. It was shown that in contrast to the moderately heterogeneous distribution achieved with wet granulation in Isoptin SR, the extrusion process yields rather homogeneous distribution for all major ingredients, especially for the API and the Na alginate matrix. High magnification studies revealed that the active ingredient formed mostly solid solution (or at least colloidal dispersion) with the alginate polymer, while some part is present as few (or sub-) micron sized particles.

Considering the results shown in this study, it can be stated that even though not the whole amount of API was dispersed in the polymer matrix, the remaining small crystals are also well protected by the alginate surrounding, preventing enhanced dissolution even if high amount of ethanol is present in the dissolution media. This proves that melt extrusion is a useful procedure to manufacture sustained release products which can retain their dissolution profile under a wider range of conditions than the conventionally prepared products.

Acknowledgements

The research was supported by the OTKA Research Fund (code K76346), ERA Chemistry (code NN 82426), W2Plastics EU7 Project (code 212782), and the Hungarian project TECH_08-A4/2-2008-0142. This work is connected to the scientific program of the "Development of quality-oriented and harmonized R + D + I strategy and functional model at BME" project. This project is supported by the New Széchenyi Plan (Project ID: TÁMOP-4.2.1/B-09/1/KMR-2010-0002).

References

Amigo, J.M., 2010. Practical issues of hyperspectral imaging analysis of solid dosage forms. Anal. Bioanal. Chem. 398, 93–109.
Breitenbach, J., Schrof, W., Neumann, J., 1999. Confocal Raman-spectroscopy: analytical approach to solid dispersions and mapping of drugs. Pharm. Res. 16, 1109–1113.
Chan, K.L.A., Hammond, S.V., Kazarian, S.G., 2003. Applications of attenuated total reflection infrared spectroscopic imaging to pharmaceutical formulations. Anal. Chem. 75, 2140–2146.
Clarke, F., 2004. Extracting process-related information from pharmaceutical dosage forms using near infrared microscopy. Vib. Spectrosc. 34, 25–35.
de Juan, A., Tauler, R., 2006. Multivariate curve resolution (MCR) from 2000: progress in concepts and applications. Crit. Rev. Anal. Chem. 36, 163–176.
de Juan, A., Maeder, M., Hancewicz, T., Tauler, R., 2008. Use of local rank-based spatial information for resolution of spectroscopic images. J. Chemom. 22, 291–298.
Docoslis, A., Huszarik, K.L., Papageorgiou, G.Z., Bikiaris, D., Stergiou, A., Georgarakis, E., 2007. Characterization of the distribution, polymorphism, and stability of nimodipine in its solid dispersions in polyethylene glycol by micro-Raman spectroscopy and powder X-ray diffraction. AAPS J. 9, E361–E370.
Duponchel, L., Elmi-Rayaleh, W., Ruckebusch, C., Huvenne, J.P., 2003. Multivariate curve resolution methods in imaging spectroscopy: influence of extraction methods and instrumental perturbations. J. Chem. Inf. Comput. Sci. 43, 2057–2067.
Furuyama, N., Hasegawa, S., Hamaura, T., Yada, S., Nakagami, H., Yonemochi, E., Terada, K., 2008. Evaluation of solid dispersions on a molecular level by the Raman mapping technique. Int. J. Pharm. 361, 12–18.
Gan, F., Hopke, P.K., 2003. New convergence criterion for multi-variable curve resolution. Anal. Chim. Acta 495, 195–203.
Gendrin, C., Roggo, Y., Collet, C., 2008a. Pharmaceutical applications of vibrational chemical imaging and chemometrics: a review. J. Pharm. Biomed. Anal. 48, 533–553.
Gendrin, C., Roggo, Y., Collet, C., 2008b. Self-modelling curve resolution of near infrared imaging data. J. Near Infrared Spectrosc. 16, 151–157.
Gordon, K.C., McGoverin, C.M., 2010. Raman mapping of pharmaceuticals. Int. J. Pharm., doi:10.1016/j.ijpharm.2010.12.030.
Gowen, A.A., O'Donnell, C.P., Cullen, P.J., Bell, S.E.J., 2008. Recent applications of chemical imaging to pharmaceutical process monitoring and quality control. Eur. J. Pharm. Biopharm. 69, 10–22.

Jaumot, J., Gargallo, R., de Juan, A., Tauler, R., 2005. A graphical user-friendly interface for MCR–ALS: a new tool for multivariate curve resolution in MATLAB. Chemom. Intell. Lab. Syst. 76, 101–110.

Jaumot, J., Tauler, R., 2010. MCR-BANDS: a user friendly MATLAB program for the evaluation of rotation ambiguities in multivariate curve resolution. Chemom. Intell. Lab. Syst. 103, 96–107.

Karavas, E., Georgarakis, M., Docoslis, A., Bikiaris, D., 2007. Combining SEM TEM, and micro-Raman techniques to differentiate between the amorphous molecular level dispersions and nanodispersions of a poorly water-soluble drug within a polymer matrix. Int. J. Pharm. 340, 76–83.

Lin, W.-Q., Jiang, J.-H., Yang, H.-F., Ozaki, Y., Shen, G.-L., Yu, R.-Q., 2006. Characterization of chloramphenicol palmitate drug polymorphs by Raman mapping with multivariate image segmentation using a spatial directed agglomeration clustering method. Anal. Chem. 78, 6003–6011.

Nagy, Z.K., Nyúl, K., Wágner, I., Molnár, K., Marosi, G., 2010. Electrospun water soluble polymer mat for ultrafast release of donepezil HCl. Expr. Polym. Lett. 4, 763–772.

Puchert, T., Lochmann, D., Menezes, J.C., Reich, G., 2010. Near-infrared chemical imaging (NIR-CI) for counterfeit drug identification – a four-stage concept with a novel approach of data processing (linear image signature). J. Pharm. Biomed. Anal. 51, 138–145.

Rajkó, R., István, K., 2005. Analytical solution for determining feasible regions of self-modeling curve resolution (SMCR) method based on computational geometry. J. Chemometr. 19, 448–463.

Rajkó, R., 2009. Computation of the range (band boundaries) of feasible solutions and measure of the rotational ambiguity in self-modeling/multivariate curve resolution. Anal. Chim. Acta 645, 18–24.

Ravn, C., Skibsted, E., Bro, R., 2008. Near-infrared chemical imaging (NIR-CI) on pharmaceutical dosage forms – comparing common pharmaceutical approaches. J. Pharm. Biomed. Anal. 48, 554–561.

Roth, W., Setnik, B., Zietsch, M., Burst, A., Breitenbach, J., Sellers, E., Brennan, D., 2009. Ethanol effects on drug release from verapamil Meltrex®, an innovative melt extruded formulation. Int. J. Pharm. 368, 72–75.

Šašić, S., Clark, D.A., Mitchell, J.C., Snowden, M.J., 2004. A comparison of Raman chemical images produced by univariate and multivariate data processing – a simulation with an example from pharmaceutical practice. Analyst 129, 1001–1007.

Šašić, S., 2007. An in-depth analysis of Raman and near-infrared chemical images of common pharmaceutical tablets. Appl. Spectrosc. 61, 239–250.

Šašić, S., 2010. Determining the coating thickness of tablets by chiseling and image analysis. Int. J. Pharm. 397, 109–115.

Streubel, A., Siepmann, J., Dashevsky, A., Bodmeier, R., 2000. pH-independent release of a weakly basic drug from water-insoluble and -soluble matrix tablets. J. Control. Release 67, 101–110.

Tauler, R., 2001. Calculation of maximum and minimum band boundaries of feasible solutions for species profiles obtained by multivariate curve resolution. J. Chemometr. 15, 627–646.

Vajna, B., Farkas, I., Szabó, A., Zsolt, Z., Marosi, G., 2010. Raman microscopic evaluation of technology dependent structural differences in tablets containing imipramine model drug. J. Pharm. Biomed. Anal. 51, 30–38.

Vajna, B., Patyi, G., Nagy, Z., Bódis, A., Marosi, G. Comparison of chemometric methods in the analysis of pharmaceuticals with hyperspectral Raman imaging. J. Raman Spectrosc. in press. doi:10.1002/jrs.2943.

Windig, W., Keenan, M.R., 2011. Angle-constrained alternating least squares. Appl. Spectrosc. 65, 349–357.

Zhang, L., Henson, M.J., Sekulic, S.S., 2005. Multivariate data analysis for Raman imaging of a model pharmaceutical tablet. Anal. Chim. Acta 545, 262–278.